SCIENTIFIC REP🞄RTS

Electronic Structure of the Kitaev Material α-RuCl$_3$ Probed by Photoemission and Inverse Photoemission Spectroscopies

Soobin Sinn[1,2], Choong Hyun Kim[1,2], Beom Hyun Kim[3,4], Kyung Dong Lee[5], Choong Jae Won[5], Ji Seop Oh[1,2], Moonsup Han[6], Young Jun Chang[6], Namjung Hur[5], Hitoshi Sato[7], Byeong-Gyu Park[8], Changyoung Kim[1,2], Hyeong-Do Kim[1,2] & Tae Won Noh[1,2]

Recently, α-RuCl$_3$ has attracted much attention as a possible material to realize the honeycomb Kitaev model of a quantum-spin-liquid state. Although the magnetic properties of α-RuCl$_3$ have been extensively studied, its electronic structure, which is strongly related to its Kitaev physics, is poorly understood. Here, the electronic structure of α-RuCl$_3$ was investigated by photoemission (PE) and inverse-photoemission (IPE) spectroscopies. The band gap was directly measured from the PE and IPE spectra and was found to be 1.9 eV, much larger than previously estimated values. Local density approximation (LDA) calculations showed that the on-site Coulomb interaction U could open the band gap without spin-orbit coupling (SOC). However, the SOC should also be incorporated to reproduce the proper gap size, indicating that the interplay between U and SOC plays an essential role. Several features of the PE and IPE spectra could not be explained by the results of LDA calculations. To explain such discrepancies, we performed configuration-interaction calculations for a RuCl$_6^{3-}$ cluster. The experimental data and calculations demonstrated that the $4d$ compound α-RuCl$_3$ is a $J_{eff}=1/2$ Mott insulator rather than a quasimolecular-orbital insulator. Our study also provides important physical parameters required for verifying the proposed Kitaev physics in α-RuCl$_3$.

The honeycomb Kitaev model has attracted significant attention as a feasible model for a quantum-spin-liquid ground state[1–5]. In this model, a strong spin-orbit coupling (SOC) plays a critical role because it provides a bond-direction-dependent exchange interaction that results in spin frustration. Various transition-metal compounds, including Na$_2$IrO$_3$ and Li$_2$IrO$_3$, have been investigated for possible realization of the Kitaev model[6–8]. These materials contain $5d$-transition-metal Ir ions that exhibit a large SOC strength λ_{SOC} of ~0.4 eV[9].

α-RuCl$_3$ has recently been added to the list of Kitaev candidates despite the comparatively modest SOC in the $4d$ Ru ion (λ_{SOC} ~ 0.13 eV)[10]. The honeycomb lattice of the system is almost perfect, with an Ru–Cl–Ru angle of approximately 90°[11,12]. This near-perfect lattice makes the system ideal for achieving the Kitaev ground state[1–4] despite the relatively weak SOC. Numerous experimental studies involving Raman spectroscopy[13,14] or neutron scattering[10] have indicated that α-RuCl$_3$ may be close to the Kitaev spin-liquid ground state. To distinguish the interesting Kitaev quantum physics from other classical spin fluctuations, determining the accurate values of physical parameters related to the Kitaev physics, possibly from electronic structure studies, is important. However, there are still some controversies regarding the electronic structure of α-RuCl$_3$. The magnitude and nature of the band gap remain controversial. An early Hall-effect study of α-RuCl$_3$ claimed that the band gap

[1]Center for Correlated Electron Systems, Institute for Basic Science (IBS), Seoul 08826, Republic of Korea. [2]Department of Physics and Astronomy, Seoul National University (SNU), Seoul 08826, Republic of Korea. [3]Computational Condensed Matter Physics Laboratory, RIKEN, Wako, Saitama 351-0198, Japan. [4]Interdisciplinary Theoretical Science (iTHES) Research Group, RIKEN, Wako, Saita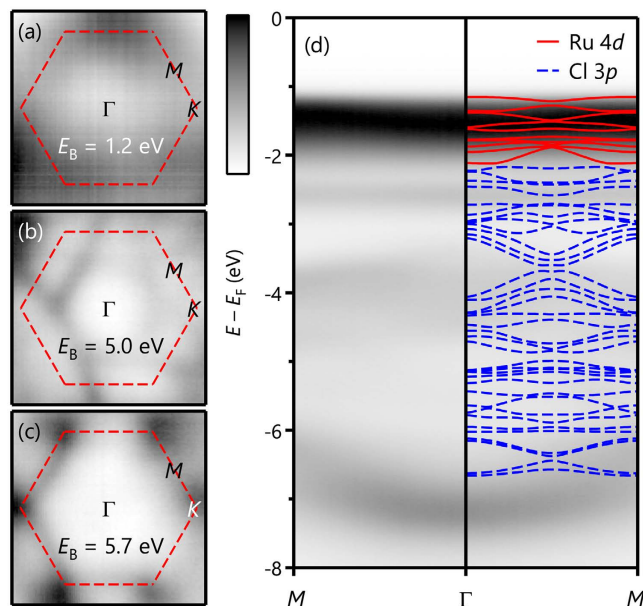ma 351-0198, Japan. [5]Department of Physics, Inha University, Incheon 22212, Republic of Korea. [6]Department of Physics, University of Seoul, Seoul 02504, Republic of Korea. [7]Hiroshima Synchrotron Radiation Center, Hiroshima University, Kagamiyama 2-313, Higashi-Hiroshima 739-0046, Japan. [8]Pohang Accelerator Laboratory, Pohang University of Science and Technology, Pohang 37673, Republic of Korea. Correspondence and requests for materials should be addressed to H.-D.K. (email: hdkim6612@snu.ac.kr)

Figure 1. Momentum-dependent electronic structure of α-RuCl$_3$. ARPES constant-energy maps at different binding energies of (**a**) 1.2 eV, (**b**) 5.0 eV, and (**c**) 5.7 eV. Red-dashed hexagons indicates the Brillouin zone of α-RuCl$_3$. (**d**) Band dispersions from ARPES along the $M\Gamma M$ line. Calculated bands by LDA + SOC + U ($U - J_H = 4.5$ eV) are depicted on the right-hand side of (**d**). Red solid lines and blue dashed lines represent Ru 4d and Cl 3p bands, respectively. Note that the existence of a flat band at -2.5 eV and the clear separation between Ru 4d bands and Cl 3p bands are not reproduced in the LDA + SOC + U calculations.
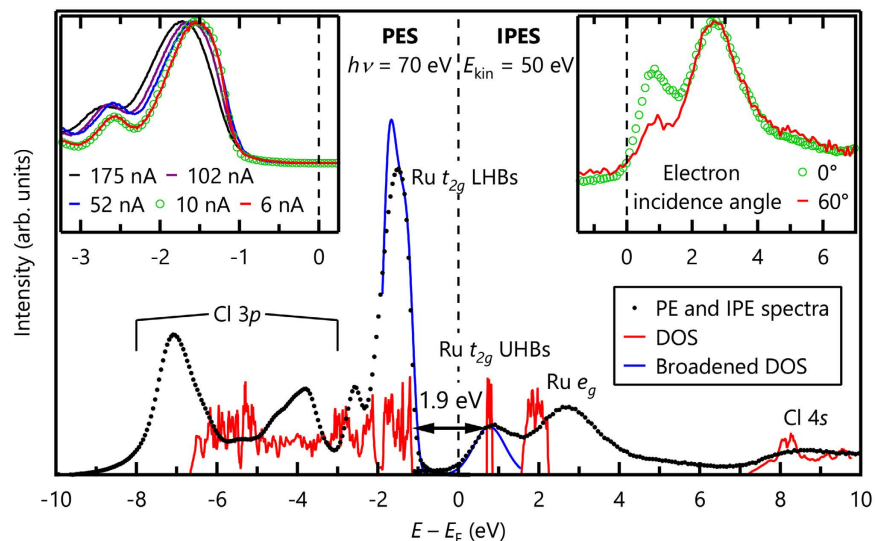
should be approximately 0.3 eV[15]. Optical studies found an optical gap of 0.2 eV[16] that was later revised to 1.0 eV[17]. Recently, an angle-resolved photoemission spectroscopy (ARPES) study showed that the Fermi level E_F is located 1.2 eV above the valence band maximum, suggesting that the band gap should be larger than 1.2 eV[18]. There are two possible insulating mechanisms for a spin-orbit-coupled t_{2g}^5 honeycomb system[19]: A $J_{eff} = 1/2$ Mott insulator[20] and a quasimolecular-orbital band insulator[21]. Whereas the model presumes the $J_{eff} = 1/2$ Mott state[1], this state has not been experimentally confirmed for this system. Moreover, the physical parameters characterizing the electronic structure and interactions that constitute a key input into the theoretical descriptions of the unconventional magnetism have not yet been determined.

Here, we describe our experimental and theoretical efforts to understand the electronic structure of α-RuCl$_3$ using both photoemission (PE) and inverse photoemission (IPE) spectroscopies. We observed a band gap of approximately 1.9 eV, much larger than the previously reported values. Local density approximation (LDA) calculations also reveal that the interplay between SOC and electron correlation plays an important role in determining the insulating ground state of α-RuCl$_3$. However, some features of the PE and IPE spectra could not be fully explained by the band calculations, implying a strongly correlated ground state. To explain such detailed features, we performed configuration-interaction (CI) calculations for a RuCl$_6^{3-}$ cluster and determined the microscopic parameters relevant to Kitaev physics.

Results and Discussion

The underlying honeycomb symmetry of α-RuCl$_3$ can be manifested in the constant-energy maps of the ARPES data. Figures 1(a)-(c) show constant-energy maps at the binding energies of $E_B = 1.2$, 5.0, and 5.7 eV, respectively. At $E_B = 1.2$ eV, the crystal symmetry is not clearly resolved, probably because of the negligible dispersions of the Ru t_{2g} bands. At the higher binding energies, the maps show a six-fold symmetry originating from the dispersive Cl 3p bands. These constant-energy maps confirm the high quality of our sample surfaces investigated.

ARPES spectra along the $M\Gamma M$ line in Fig. 1(d) show the nearly flat Ru 4d bands near the E_F and the dispersive Cl 3p bands. Most of the Ru 4d bands are located between -1.0 and -3.0 eV. In an enlarged view of the Ru 4d bands near -1.5 eV, their dispersions are estimated to be approximately 0.1 eV or smaller. By contrast, the Cl 3p bands are located between -3.5 and -7.5 eV and are well separated from the Ru 4d bands. Compared to the Ru 4d bands, the Cl 3p bands are highly dispersive. Overall, our ARPES spectra are consistent with recently reported ARPES results[18,22]. Note that the energy differences between the five Ru t_{2g} bands (<0.2 eV) are much smaller than the band gap (>1.2 eV). These results imply that α-RuCl$_3$ is not a quasimolecular-orbital insulator; otherwise, the t_{2g} band distances and the band gap would exhibit a common energy scale of d-d hopping[21]. For comparison, we overlaid the band dispersions based on the results of LDA + SOC + U calculations; the result is shown in the right-hand side of Fig. 1(d). The red and blue solid lines correspond to the Ru t_{2g} bands and the Cl 3p bands, respectively. The calculations also support our finding that the flat Ru 4d and the dispersive Cl 3p bands are located near and much below the E_F, respectively. Despite this success, some discrepancies between the ARPES spectra and the calculation results exist, as discussed below.
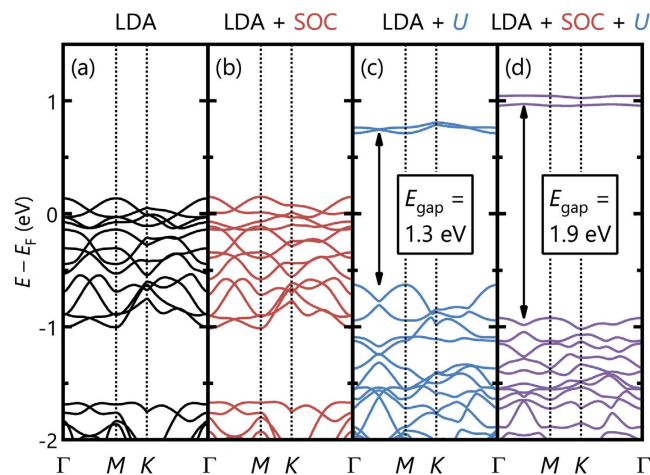
Figure 2. PE and IPE spectra of α-RuCl$_3$. The red and blue solid lines represent the density of states and the broadened one from LDA + SOC + U calculations, respectively. By comparing the experimental and theoretical results, we estimated the size of the band gap to be approximately 1.9 eV. Note that the crystal field splitting is underestimated in the LDA + SOC + U calculations. The top-left and top-right insets show source-flux dependence in PE and IPE spectra, respectively. The PE and IPE spectra are measured at the conditions (10 nA and electron incidence angle = 0°) under which charging effects are negligible.

To resolve the controversy regarding the size of the band gap, we used a combination of angle-integrated PE and IPE spectroscopies. Note that the PE and IPE spectra contain information about the density of states of the occupied and unoccupied bands, respectively. Therefore, the combination of PE and IPE spectroscopies has been established as the most direct method for determining an electronic energy gap[23]. To avoid possible sample charging effects, we adjusted source fluxes for both ARPES and IPE experiments as shown in the insets of Fig. 2 (see the Method section for a detailed description). The black dots in Fig. 2 show both the PE and IPE spectra of α-RuCl$_3$. The PE spectrum was obtained from the ARPES data of Fig. 1(d) by integrating over the momentum. On the basis of the arguments for Fig. 1(d), we assign the peak at approximately -1.5 eV to the Ru t_{2g} antibonding lower Hubbard bands (LHBs). The two strong peaks at approximately -4.0 and -7.0 eV should originate from the Cl $3p$ nonbonding and bonding bands, respectively. The right-hand side of Fig. 2 shows an IPE spectrum. Two prominent peaks near the E_F are assigned to the Ru t_{2g} upper Hubbard bands (UHBs) and Ru e_g bands. The crystal-field splitting $10Dq$, which is the energy separation between the Ru t_{2g} UHBs and e_g bands, is estimated to be approximately 2.2 eV. This value is similar to that observed in an x-ray absorption spectrum[16].

We estimate the band gap of α-RuCl$_3$ to be 1.9 eV, which is much larger than the values reported in earlier studies[15-18]. In principle, the size of the band gap should correspond to the energy range of zero intensity in PE and IPE spectra. However, the range of zero intensity is reduced because of hole or electron lifetime and experimental spectral broadening. Usually, the position of a band edge is experimentally determined by the half maximum or by the intersection point of a linear extrapolation of the leading edge. The size of the errors for those methods is approximately a half of the experimental resolution. If the resolution is not good enough as in the IPE spectrum, the error will be comparable to the band-gap size. To reduce the error, we utilized the density of states from the LDA + SOC + U calculations, which was broadened by experimental resolutions as shown in blue lines of Fig. 2. To reproduce the PE and IPE spectra near the E_F, we used $U - J_H = 4.5$ eV in the calculations. (J_H is the Hund's coupling). As shown in Fig. 2, the LDA + SOC + U can explain both the valence and conduction bands near the E_F reasonably well. On the basis of this comparison, we assigned the valence band maximum and the conduction band minimum. Then, the band gap of α-RuCl$_3$ should be approximately 1.9 eV. Note that this magnitude is clearly much higher than the 0.3 eV value obtained via a Hall-effect study[15], and also higher than the 1.0 eV value from recent optical studies[17]. The former may be related with an activation gap due to defect states, and the latter implies strong exciton effect that is observed in alkali halides[24] and other transition-metal compounds[25].

We found that the interplay between the Coulomb interaction U and SOC is essential for understanding the physics of α-RuCl$_3$. To clarify the roles of these effects, we performed LDA calculations with and without the U and SOC terms. Figures 3(a)–(d) display the results of LDA, LDA + SOC, LDA + U, and LDA + SOC + U calculations. As shown in Fig. 3(a), in the absence of U and SOC, the partially filled Ru bands with t_{2g}^5 electrons should result in a metallic ground state. As shown in Fig. 3(b), the system still remains metallic when SOC is included in the calculations. Nevertheless, the narrow t_{2g} bands repel each other because of SOC, resulting in an apparent total t_{2g} bandwidth broadening, as reported previously[26]. By contrast, as shown in Fig. 3(c), the LDA + U results predict a gapped electronic structure, indicating the prime importance of the Coulomb interaction for the insulating nature of α-RuCl$_3$. However, the predicted gap size is only approximately 1.3 eV. We can properly describe the observed energy gap value of 1.9 eV only when we include both SOC and U. The large enhancement of the gap

Figure 3. Electronic band structures of α-RuCl$_3$ by changing U and SOC. (a) LDA, **(b)** LDA + SOC, **(c)** LDA + U, and **(d)** LDA + SOC + U calculations. Note that the band-gap value of approximately 1.9 eV can be explained only when both U and SOC terms are included.

U	J_H	λ_{SOC}	$10Dq$	Δ	$t_{pd\sigma}$	$t_{pd\pi}$
4.35	0.35	0.13	2.2	5.0	1.90	−0.90

Table 1. Physical parameters of CI calculations. Units are in eV. The parameters were determined by reproducing the experimental PE and IPE spectra in Fig. 2 with CI calculations.
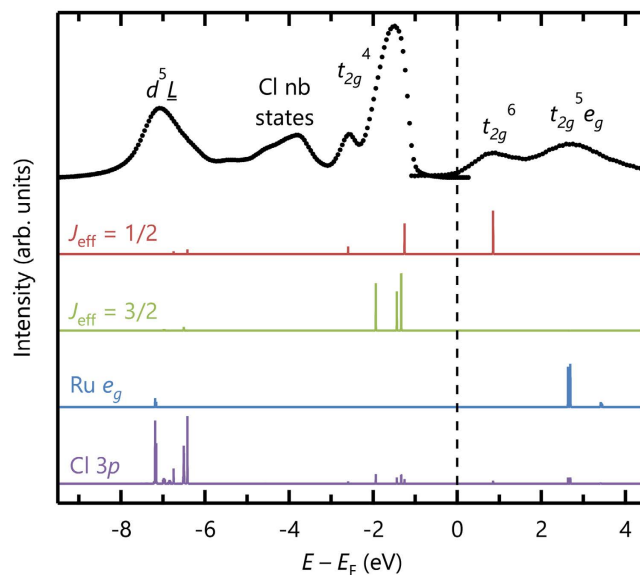
size by 0.6 eV due merely to the introduction of a small SOC of 0.13 eV indicates that SOC plays a crucial role in the electronic structure of α-RuCl$_3$, especially near the Fermi level[27].

Although the PE and IPE spectra can be explained reasonably well by the LDA + SOC + U calculation results, some discrepancies still exist. In Figs 1(d) and 2, a sharp nondispersive peak that cannot be explained by the calculations is observed at approximately −2.5 eV. The orbital character of this peak appears to be Ru 4d because its intensity change with varied photon energies is similar to those of the main Ru t_{2g} bands[22]. Moreover, the clear separation between the Ru 4d and the Cl 3p bands in the ARPES spectrum cannot be reproduced in the calculations. As shown in the IPE spectrum of Fig. 2, the size of the crystal-field splitting is also underestimated in the LDA + SOC + U results.

To gain further insights, we carried out CI calculations for a single RuCl$_6$$^{3-}$ cluster, in which we considered the Ru 4d and the Cl 3p bonding orbitals while taking the full multiplet structures into account. Whereas a local cluster calculation study of the α-RuCl$_3$ has been reported in the literature, this work only considered the d^5 ground state multiplets that are not directly related to the PE and IPE spectra[28]. To reduce the dimension of the Hilbert space, the Cl nonbonding states at approximately −4 eV are not considered in our calculations. The relevant Hamiltonian has numerous parameters, including U, J_H, λ_{SOC}, $10Dq$, charge-transfer energy Δ for the excitation from the Cl 3p to Ru t_{2g} orbitals, and Slater-Koster parameters $t_{pd\sigma}$ and $t_{pd\pi}$. However, many of these parameters can be determined unambiguously, i.e., the λ_{SOC} value was adopted from an inelastic neutron scattering study[10], the $10Dq$ value from the energy difference between the Ru t_{2g} UHBs and the Ru e_g peak, and the Δ value from the energy difference between the Cl nonbonding states and the Ru t_{2g} UHBs. In most transition-metal compounds, $t_{pd\sigma}$ is approximately two times larger than $t_{pd\pi}$[29]. Then, the values of the remaining three parameters, U, J_H, and $t_{pd\pi}$, can be obtained with minor errors by fitting the band gap, the −2.5 eV peak position, and the position of the $d^5\underline{L}$ final states at approximately −7 eV. The obtained parameter values are listed in Table 1. Note that the magnitudes of U, J_H, and Δ are difficult to determine without spectroscopic data because of dynamical screening[30,31].

Our CI calculations can explain the spectral features of the PE and IPE spectra that were difficult to explain on the basis of LDA + SOC + U calculations. As shown in Fig. 4, the positions of the energy levels determined from the CI calculations are in good agreement with the peak positions in the PE and IPE spectra. Despite the moderate SOC, the electronic structure of α-RuCl$_3$ is governed by J_{eff} = 1/2 physics because the electronic energy gap is determined by excited hole and electron states that solely originate from the J_{eff} = 1/2 state. Among five multiplets of t_{2g}^4 configurations, curious −2.5 eV peak not explained by the band calculations emerges as a J_{eff} = 1/2 state. The unusual high-binding energy of J_{eff} = 1/2 state originates from the strong Hund's coupling of Ru d orbitals (refer to the Supplemental Material of ref. 19 for a detailed description). The agreement between the J_{eff} = 1/2 nature and a large U signifies that the 4d compound α-RuCl$_3$ has a strong local nature and a relativistic Mott ground state instead of the quasimolecular-orbital insulating state[19].

The values of physical parameters obtained from the CI calculations can be utilized to study the Kitaev physics in α-RuCl$_3$. The strengths of the Heisenberg (J), Kitaev (K), and off-diagonal (Γ) exchange interactions in the Heisenberg-Kitaev model are easily obtained[2,3,32] from our values for the physical parameters listed in Table 1.

Figure 4. Comparison of PE and IPE spectra obtained experimentally and from CI calculations for (**a**) $RuCl_6^{3-}$ cluster. Spectral weights from CI calculations are shown separately by their spin-orbital characters in the ground state. The electronic energy gap is determined solely by excited states from the $J_{eff}=1/2$ state. Note that nonbonding Cl $3p$ orbitals are not included in the calculations; thus, no peak is observed at approximately $-4\,eV$.

The single shortcoming of our approach is that our CI calculations were performed on a single-site $RuCl_6^{3-}$ cluster and therefore did not include the direct d-d hopping terms between the nearest-neighbor Ru ions. To obtain the exchange interaction terms, we adopted the values of the d-d hopping parameters $t_{dd\sigma}$ and $t_{dd\pi}$ from a recent theoretical study[33]. The exchange strengths of J, K, and Γ are then determined to be -0.7, -1.6, and $1.5\,meV$, respectively. The magnitudes of these values are much smaller than those estimated from inelastic neutron scattering experiments[10] but are similar to those obtained from recent quantum chemistry calculations based on an assumed $P3_112$ structure[28]. To be more precise, performing the CI calculations with a full set of Ru $4d$ orbitals for a multi-site cluster is highly desirable[19]; however, this approach requires a much larger Hilbert space.

Conclusion

In conclusion, we investigated the electronic structure of the Kitaev candidate material α-$RuCl_3$. By combining both photoemission and inverse photoemission studies, we directly measured a band gap of $1.9\,eV$ in α-$RuCl_3$; this band gap is much larger than values reported previously. We also showed that the interplay between the electron correlation and SOC plays a crucial role in determining the nature of the Mott insulating ground state of α-$RuCl_3$. By taking into account the many-body effects using CI calculations for a $RuCl_6^{3-}$ cluster, we obtained the physical parameters and exchange-interaction strengths of the Heisenberg-Kitaev model. The obtained parameters will provide a useful guide for the synthesis of Kitaev materials with the quantum-spin-liquid state. For example, the application of pressure or strain could be a strategy for achieving this goal. The evolution of the system due to the perturbations on the Kitaev phase diagram strongly depends on details of the parameters obtained in this study.

Methods

Experiments. Single-crystalline samples of α-$RuCl_3$ were grown by the self-chemical vapor transport method. Their crystallinity was confirmed by Laue diffraction. All samples were cleaved *in situ* for ARPES and IPE measurements. ARPES measurements were performed at the Beamline 4A1 of Pohang Light Source. ARPES spectra were obtained at the photon energy of $h\nu = 70\,eV$ and with a total energy resolution of $50\,meV$. During the measurements, the sample temperature was maintained at $280\,K$ under a vacuum of $3 \times 10^{-11}\,Torr$. IPE measurements were carried out at HiSOR[34,35]. The incident electron kinetic energy was set to $50\,eV$ and an energy resolution was $0.9\,eV$. The sample temperature was $340\,K$ under a vacuum of $3 \times 10^{-10}\,Torr$. IPE spectra were obtained in the normal incidence mode. The angular divergence of the electron beam was approximately $4°$, corresponding to approximately one-third the length of the ΓK line. The Fermi levels and total experimental resolutions of ARPES and IPE spectra were determined by measuring the Fermi edge of Au electrically contacted to the sample. We checked sample charging effects in both PE and IPE spectra by varying source fluxes. The results are shown in the insets of Fig. 2. In PE spectra, when the photon flux is smaller than $10\,nA$, the spectral shift and the line-shape change due to charging becomes negligible. In IPE spectra, we changed the electron flux per unit area by changing the electron incident angle. As shown in the top-right inset of Fig. 2, the shift of the IPE spectrum was negligible even when the incidence electron density on the sample surface is decreased by approximately two times. The PE and IPE spectra in the main text were taken at $10\,nA$ and the electron incidence angle of $0°$, respectively.

Theory.   To calculate the band structure, we used the density functional theory code OPENMX (http://www.openmx-square.org) with a zigzag magnetic ordering that was reported to occur in α-RuCl$_3$[11,36]. In the LDA $+ U$ and LDA $+$ SOC $+ U$ calculations, the $U - J_H$ value of 4.5 eV was used to reproduce the PE and IPE spectra near the E_F. To explain the fine details of the PE and IPE spectra, we also performed CI calculations[37] for a local RuCl$_6{}^{3-}$ cluster while neglecting the nonbonding Cl $3p$ molecular orbitals. We solved the Hamiltonian for a five-hole system using the Lanczos exact diagonalization method and calculated the one-particle Green's functions by spanning the eigenvalues of four- and six-hole systems using the band Lanczos method[38].

References

1. Chaloupka, J., Jackeli, G. & Khaliullin, G. Kitaev-Heisenberg Model on a Honeycomb Lattice: Possible Exotic Phases in Iridium Oxides A$_2$IrO$_3$. *Physical Review Letters* **105,** 027204 (2010).
2. Rau, J. G., Lee, E. K.-H. & Kee, H.-Y. Generic Spin Model for the Honeycomb Iridates beyond the Kitaev Limit. *Physical Review Letters* **112,** 077204 (2014).
3. Chaloupka, J., Jackeli, G. & Khaliullin, G. Zigzag Magnetic Order in the Iridium Oxide Na$_2$IrO$_3$. *Physical Review Letters* **110,** 097204 (2013).
4. Chaloupka, J. & Khaliullin, G. Hidden symmetries of the extended Kitaev-Heisenberg model: Implications for the honeycomb-lattice iridates A$_2$IrO$_3$. *Physical Review B* **92,** 024413 (2015).
5. Kitaev, A. Anyons in an exactly solved model and beyond. *Annals of Physics* **321,** 2 (2006).
6. Singh, Y. *et al.* Relevance of the Heisenberg-Kitaev Model for the Honeycomb Lattice Iridates A$_2$IrO$_3$. *Physical Review Letters* **108,** 127203 (2012).
7. Choi, S. K. *et al.* Spin Waves and Revised Crystal Structure of Honeycomb Iridate Na$_2$IrO$_3$. *Physical Review Letters* **108,** 127204 (2012).
8. Chun, S. H. *et al.* Direct evidence for dominant bond-directional interactions in a honeycomb lattice iridate Na$_2$IrO$_3$. *Nature Physics* **11,** 462 (2015).
9. Kim, B. H., Khaliullin, G. & Min, B. I. Electronic excitations in the edge-shared relativistic Mott insulator: Na$_2$IrO$_3$. *Physical Review B* **89,** 081109 (2014).
10. Banerjee, A. *et al.* Proximate Kitaev quantum spin liquid behaviour in a honeycomb magnet. *Nature Materials* **15,** 733 (2016).
11. Johnson, R. D. *et al.* Monoclinic crystal structure of α-RuCl$_3$ and the zigzag antiferromagnetic ground state. *Physical Review B* **92,** 235119 (2015).
12. Cao, H. B. *et al.* Low-temperature crystal and magnetic structure of α-RuCl$_3$. *Physical Review B* **93,** 134423 (2016).
13. Sandilands, L. J., Tian, Y., Plumb, K. W., Kim, Y. J. & Burch, K. S. Scattering Continuum and Possible Fractionalized Excitations in α-RuCl$_3$. *Physical Review Letters* **114,** 147201 (2015).
14. Nasu, J., Knolle, J., Kovrizhin, D. L., Monome, Y. & Moessner, R. Fermionic response from fractionalization in an insulating two-dimensional magnet. *Nature Physics* **12,** 912 (2016).
15. Rojas, S. & Spinolo, G. Hall Effect in α-RuCl$_3$. *Solid State Communications* **48,** 349 (1983).
16. Plumb, K. W. *et al.* α-RuCl$_3$: A spin-orbit assisted Mott insulator on a honeycomb lattice. P*hysical Review B* **90,** 041112 (2014).
17. Sandilands, L. J. *et al.* Spin-orbit excitations and electronic structure of the putative Kitaev magnet α-RuCl$_3$. *Physical Review B* **93,** 075144 (2016).
18. Zhou, X. *et al.* Angle-resolved photoemission study of the Kitaev candidate α-RuCl$_3$. *Physical Review B* **94,** 161106 (2016).
19. Kim, B. H., Shirakawa, T. & Yunoki, S. From a Quasimolecular Band Insulator to a Relativistic Mott Insulator in $t_{2g}{}^5$ Systems with a Honeycomb Lattice Structure. *Physical Review Letters* **117,** 187201 (2016).
20. Kim, B. J. *et al.* Novel $J_{eff}=1/2$ Mott State Induced by Relativistic Spin-Orbit Coupling in Sr$_2$IrO$_4$. *Physical Review Letters* **101,** 076402 (2008).
21. Mazin, I. I., Jeschke, H. O., Foyevtsova, K., Valenti, R. & Khomskii, D. I. Na$_2$IrO$_3$ as a Molecular Orbital Crystal. *Physical Review Letters* **109,** 197201 (2012).
22. Koitzsch, A. *et al.* J_{eff} Description of the Honeycomb Mott Insulator α-RuCl$_3$. *Physical Review Letters* **117,** 126403 (2016).
23. Hüfner, S. *Photoelectron Spectroscopy.* (Springer-Verlag Berlin Heidelberg, 2003).
24. Fox, M. *Optical Properties of Solids.* (Oxford University Press, 2010).
25. Matiks, Y., Horsch, P., Kremer, R. K., Keimer, B. & Boris, A. V. Exciton Doublet in the Mott-Hubbard Insulator LiCuVO$_4$ Identified by Spectral Ellipsometry. *Physical Review Letters* **103,** 187401 (2009).
26. Kim, H. S., Shankar, V. V., Catuneanu, A. & Kee, H. Y. Kitaev magnetism in honeycomb RuCl$_3$ with intermediate spin-orbit coupling. *Physical Review B* **91,** 241110 (2015).
27. Kim, W. J. *et al.* Spin-orbit coupling induced band structure change and orbital character of epitaxial IrO$_2$ films. *Physical Review B* **93,** 045104 (2016).
28. Yadav, R. *et al.* Spin-orbit excitation energies, anisotropic exchange, and magnetic phases of honeycomb α-RuCl$_3$. *arXiv*:1604.04755.
29. Harrison, W. A. *Electronic Structure and the Properties of Solids.* (Dover, 1989).
30. Deboer, D. K. G., Haas, C. & Sawatzky, G. A. Exciton satellites in photoelectron spectra. *Physical Review B* **29,** 4401 (1984).
31. Zaanen, J., Westra, C. & Sawatzky, G. A. Determination of the electronic structure of transition-metal compounds - 2*p* x-ray photoemission spectroscopy of the nickel dihalides. *Physical Review B* **33,** 8060 (1986).
32. Mazin, I. I. *et al.* Origin of the insulating state in honeycomb iridates and rhodates. *Physical Review B* **88,** 035115 (2013).
33. Kim, H.-S. & Kee, H.-Y. Crystal structure and magnetism in α-RuCl$_3$: An *ab initio* study. *Physical Review B* **93,** 155143 (2016).
34. Sato, H., Kotsugi, T., Senba, S., Namatame, H. & Taniguchi & M. UV emission spectrometer using a nonperiodic grating. *Journal of Synchrotron Radiation* **5,** 772 (1998).
35. Arita, M. *et al.* Unoccupied electronic structure of Y$_{1-x}$Ca$_x$TiO$_3$ invesigated by inverse photoemission spectroscopy. *Physical Review B* **75,** 205124 (2007).
36. Sears, J. A. *et al.* Magnetic order in α-RuCl$_3$: A honeycomb-lattice quantum magnet with strong spin-orbit coupling. *Physical Review B* **91,** 144420 (2015).
37. de Groot, F. & Kotani, A. *Core Level Spectroscopy of Solids.* (CRC Press Taylor & Francis Group, 2008).
38. Sénéchal, D. An introduction to quantum cluster methods. *arXiv*:0806.2690.

Acknowledgements

Author Contributions

S.S. and H.-D.K. conceived the work. K.D.L., C.J.W., and N.J.H. synthesized α-RuCl$_3$ crystals. S.S., J.S.O., H.-D.K., and B.-G.P. carried out the ARPES experiments, and S.S., J.S.O., H.-D.K., and H.S. performed IPE experiments. C.H.K. conducted the LDA calculations, and B.H.K. carried out the CI calculations. The research was carried out with guidance from M.H., Y.J.C., C.K., H.-D.K., and T.W.N. All authors discussed the work and commented on the manuscript.

Additional Information

Competing financial interests: The authors declare no competing financial interests.

How to cite this article: Sinn, S. *et al.* Electronic Structure of the Kitaev Material α-RuCl$_3$ Probed by Photoemission and Inverse Photoemission Spectroscopies. *Sci. Rep.* **6**, 39544; doi: 10.1038/srep39544 (2016).

Publisher's note: Springer Nature remains neutral with regard to jurisdictional claims in published maps and institutional affiliations.